VH and VM Envelopes for Spudcans Founding on a Sand Layer Overlain by Clay

S.L. Li, L. Zdravkovic*
Department of Civil and Environmental Engineering
Imperial College London

D.H. Edwards
Noble Denton Marine Services
DNV UK
** corresponding author: l.zdravkovic@imperial.ac.uk*

ABSTRACT

The combined VHM (vertical, horizontal, moment) bearing capacity envelopes for a spudcan founding on a sand layer provided in ISO 19905-1 are based on foundation yield surfaces derived from model tests of footings resting on the sand's surface. Situations are frequently encountered in practice where a spudcan penetrates through a clay layer and is founded upon an underlying sand layer. The use of bearing capacity solutions based on surface footings for such a scenario may be overly conservative as they would not account for either the contribution from the overlying clay layer, or the increased geostatic stresses within the sand layer.

This paper seeks to address this gap by conducting a parametric study using 3D geotechnical finite element analyses to examine the VH and VM bearing capacity envelopes for a circular footing founded on a sand layer overlain by a clay layer. Parametric variations include the thickness of clay overburden, depth of cavity above the footing, footing diameter and mechanical properties of both the clay and sand layers. The results are interpreted to derive the corresponding values of the horizontal and moment bearing capacity factors, C_H and C_M, that capture the beneficial increase of bearing capacity resulting from the penetration depth and the overlying clay.

KEY WORDS: Bearing capacity; footing/foundations; clay-over-sand; plasticity; finite element analysis.

INTRODUCTION

The development of offshore energy resources, first hydrocarbons and more recently electricity generated from the wind, has a significant reliance upon mobile jack-up rigs. Such rigs comprise a hull with three or more retractable legs, which typically have foundations with conical bases formed of steel plates called spudcans. The retractable legs allow the platform to be towed to the target location and positioned by tugboats, or can be self-propelled and dynamically positioned. Once at the required location, the legs are lowered to the seafloor and are proof loaded by a process of preloading or predriving. Studying the capacity of this foundation type has been of particular interest to ensure the stability of the structure when subjected to combinations of wind, wave and seismic loading and as offshore developments progress, increased structural load demands and greater foundation capacity and stiffness can be required.

The most widely used standard regarding jack-up foundation assessments, ISO 19905-1 [4], divides the assessment of the jack-up into 1) structural component of the leg, hull, spudcan and their connections, 2) The soil-structure interaction applied as an equivalent action from combinations of vertical, horizontal, static and dynamic storm load actions from extreme or stochastic events and 3) foundation modelling as a separate analysis; the latter is relevant to this study.

Macro-element models capturing the combined soil-foundation behaviour have been developed by various researchers that are similar to constitutive models used for modelling the soil in numerical analyses. Such models comprise a yield surface, flow rule, and hardening law, such as that for circular footings in clay reported in [2]. These models are beneficial because the macro-element behaviour can be incorporated into a general pushover analysis of the structure with minimal computational effort and in a fraction of time, compared to numerical analyses coupling the structure and the soil, which are computationally more expensive and time consuming. To date macro-element models have typically focused more on homogeneous soil profiles, such as sand or clay and have not yet been developed for clay overlying sand.

In the case of spudcans founding within sand, previous research work and current guidelines such as ISO 19905-1 [4] have mainly focused on the spudcans founding on the seabed surface, with either partial or full contact

being achieved, which is a reasonable assumption for homogeneous sand soil profiles. However, in many practical applications, the soil profile can comprise clay overlying sand in which the spudcans of jack-up rigs can penetrate deeper into the soil. In such cases, the foundation capacities and stiffnesses of the sand could be enhanced by beneficial depth effects and higher in-situ soil stresses. Moreover, studies on the behaviour of multi-layered soils, which are often encountered in practical applications, are typically only incorporated in the relevant guidelines by simplified methods for the vertical bearing capacity and do not provide detailed guidance for combined VHM capacities in layered soils.

A foundation's VHM envelope can be plotted that approximately traces out the onset of foundation failure. In ISO 19905-1 [4] the spudcan penetration resistance is predicted using the equations for vertical bearing capacity. The general shear bearing capacity of clays (undrained) or silica sand (drained) is used as a base case, which is then supplemented with other formulae to cover layered soil scenarios, such as clay squeezing (soft clay on stronger layer such as sand) and punch through (stronger on weaker soil layer).

The general VHM interaction envelope for both sands and clays is given by the following formula (Templeton, 2006); variables are modified to be in line with other literature [1], tracing a parabolic ellipsoid (Fig. 1).

$$\frac{M^2}{M_0^2}+\frac{H^2}{H_0^2}-16(1-a)\left(\frac{V}{V_0}\right)^2\left(1-\frac{V}{V_0}\right)^2-4a\left(\frac{V}{V_0}\right)\left(1-\frac{V}{V_0}\right)=0 \quad (1)$$

where $a=\min\{D/2.5B,1\}$, V_0, H_0, M_0 are capacities of purely vertical, horizontal and moment loading, respectively and V, H, M are current load levels. D corresponds to the depth of the spudcan's maximum bearing area below the seafloor and B corresponds to the equivalent spudcan diameter.

For a spudcan founding within sand the maximum ultimate horizontal and moment capacities are calculated as: $H_o = C_h Q_{Vnet}$ and $M_o = C_m B Q_{Vnet}$, where $C_h = 0.12$, $C_m = 0.075$ and $Q_{Vnet} = Q_V - Ap'_o$, where Q_V is the gross vertical bearing capacity of the footing, A is the plan area of the spudcan and p'_o is the overburden pressure at the depth of the maximum bearing area below the seafloor.

ISO 19905-1 [4] notes that "*For sand, the use of net capacity is conservative because it neglects the increase in capacity due to the weight of any soil on top of the spudcan which has a beneficial effect on the horizontal and moment capacities.*"

The 'a' parameter controls the transition of the VH and VM planes from parabolic at the seabed surface shallow depths to elliptical at deeper penetration depths in Equation (1). For cohesionless soil conditions, however, ISO 19905-1 [4] states that 'a' should be set to zero and further explains that "*There is currently no existing data that can be used to justify increases of horizontal and moment capacity, or change of yield surface shape, for deeply embedded spudcans in sand. The application of the yield surface calibrated to shallow penetrations is likely to be conservative for the deep penetration case*."

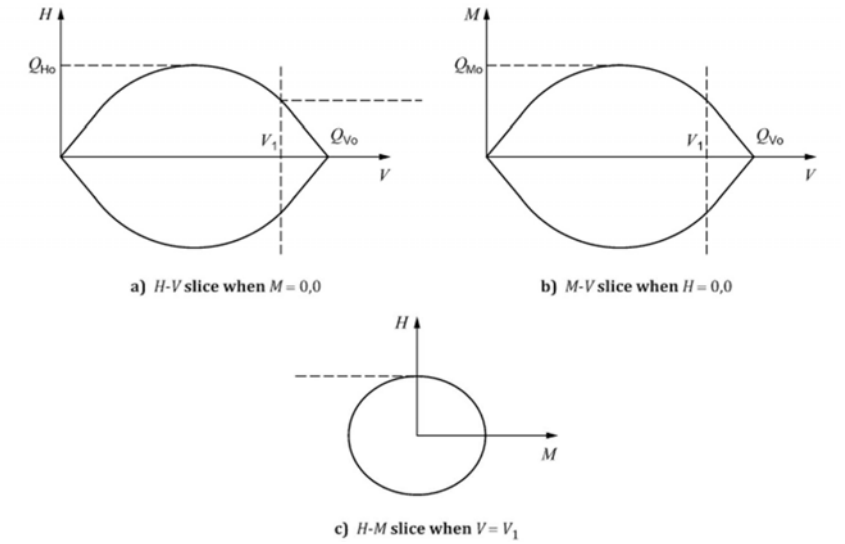

Fig. 1 Slices of the parabolic ellipsoidal VHM yield surface, from ISO 19905-1 [4]

Methodology for Defining the Yield Surface

To sweep out the yield surface, two main approaches named load probe (load control) and single side swipe test (displacement control), have been used in literature to obtain the envelope in different manners [5]. Using the VH load space as an example, a load probe test starts at the origin with zero loading and is loaded with a constant VH load gradient until failure is reached (Fig. 2), providing one data point at the yield surface. However, this approach has drawbacks as multiple tests with differing loading ratios are required, and the onset of plasticity results in a nonlinear load path, meaning the soil stiffness changes in magnitude when changing from the initial elastic state to the subsequent plastic stages and does not maintain a constant load gradient. It is therefore difficult to predict where the final state will land on, so trial and error is required to collect a sufficient number of data points in order to plot the VH surface. The benefit of the method is that it is relatively easier to converge and the final failure load can be captured accurately as a clear plateau can be seen on the load-displacement curve. On the other hand, the single side swipe test (Fig. 3) works by slowly increasing the displacement level in the other direction (horizontal in this case) while keeping the vertical displacement constant at the same initial vertical loading phase, tracing out the envelope in one continuous test. Normally, the foundation is first displaced vertically downwards until the ultimate vertical capacity is achieved, followed by the side-swipe stage which traces out the VH envelope. A second side-swipe is often performed by displacing the foundation horizontally whilst maintaining zero vertical displacement to define the envelope at low vertical load levels. However, if the swipe test sweeps out an incomplete envelope, possibly due to numerical issues and terminates prematurely, more single swipe tests can be performed at various initial vertical displacements to complete the envelope.

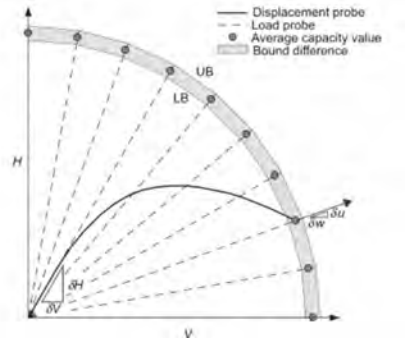

Fig. 2 Load probe test [5]

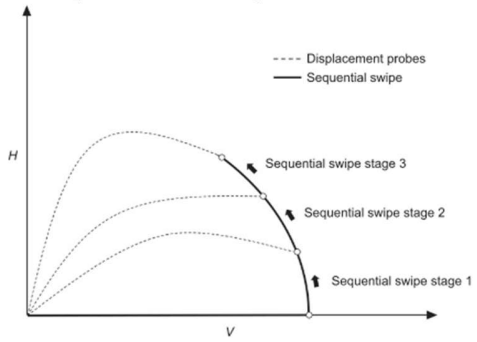

Fig. 3 Displacement side swipe test [5]

Due to the efficiency of the displacement side swipe test, it has been more common to use this approach by researchers using both physical and numerical models since the 1990s. The original tests performed by Tan (1990) [6] only include VH loading, which is named the sideswipe test. It has then been expanded to VHM load spaces by Martin and Gottardi in the late 1990s [7]. After the initial vertical loading, the other degrees of freedom (translational or rotational displacements) are held constant, to allow the quantity of interest to vary in loading. Single swipe tests of horizontal displacement (u), rotation (θ) or combinations are performed until failure to sweep out the remaining path, obtaining 2D slices in the full 3D locus as in Fig. 4 and 5 from [7, 8].

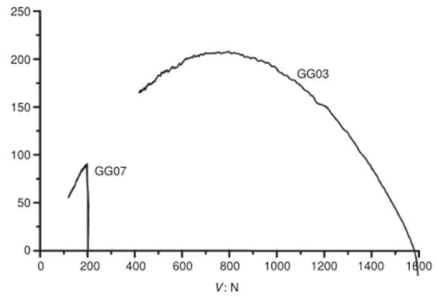

Fig. 4 VH envelope from sand model tests [7]

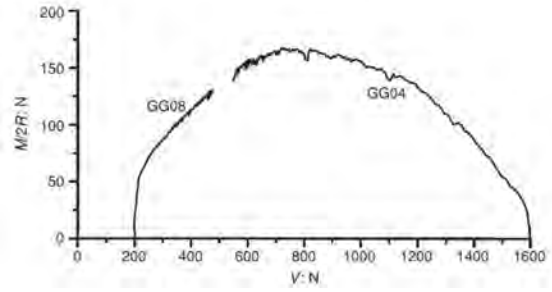

Fig. 5 VM envelope from sand model tests [7]

Layered soil failure mechanism

A finite element study of spudcan foundations in clay over sand by Wang (2021a) [9] identified the individual mechanisms for vertical, horizontal and moment loads in purely clay and clay-over-sand (Fig. 6). Clay squeezing occurs as the spudcan penetrates towards the clay-sand interface due to the constraint of the stronger underlying sand and the usual backflow mechanism requires more effort to initiate. As seen in the vertical capacity mechanisms, the displacement magnitudes in single layer clay involve a large volume of clay whereas for clay-over-sand the largest soil displacements occur between the spudcan and sand layer due to squeezing occurring. For the horizontal mechanism, the major difference is only the extra frictional forces from the sand, but not a notable difference in terms of failure mechanism. For the moment mechanism, the displacement forms a ball around the spudcan in homogeneous clay as there are no sudden changes in soil strength and a spherical plastic zone can be observed, however this mechanism is prevented by the underlying, stronger sand in the clay-sand situation. This build-up in stress mainly contributes to extra vertical and moment capacity when the footing depth reaches near the clay-sand interface compared to the single layer clay.

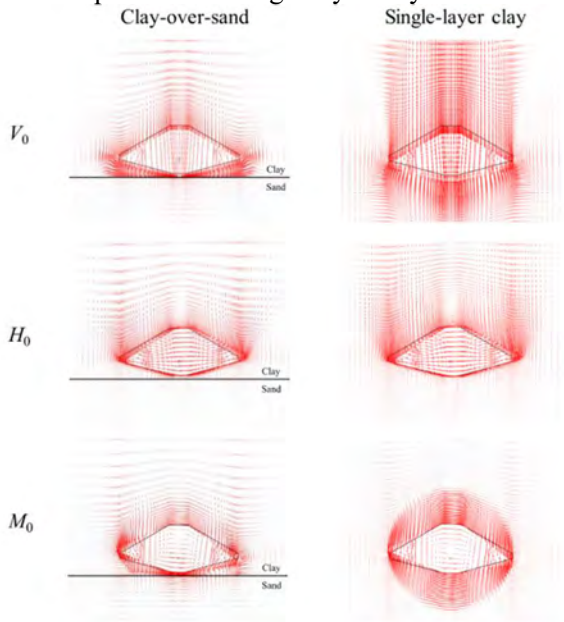

Fig. 6 Clay-over-sand and pure clay mechanisms for VHM capacities [9]

FINITE ELEMENT MODEL

Geometry

3D finite element analyses are performed with the software platform ICFEP (Imperial College Finite Element Program, [10, 11], which employs a modified Newton-Raphson method in the nonlinear solver, with an error-controlled sub-stepping stress-point algorithm. The finite element mesh is shown in Fig. 7, as a plan view (a), and as a vertical cross-section through the footing (b). The soil and the circular footing are discretised with 10480 displacement-based 20-noded hexahedral elements. The footing is thin compared to its diameter and has full adhesion with the soil underneath. Also, the footing is 'wished-in-place' in the analysis, which does not model installation effects such as backflow and penetration. These effects are considered with a simplified cavity depth, H_{cav}, calculated according to the formulations provided in ISO 19905-1 [4] based on centrifuge and model test results. The applied boundary conditions comprise zero displacements in all coordinate directions at the base of the mesh and zero horizontal displacements perpendicular to the cylindrical vertical boundary of the mesh. The load on the footing is applied through prescribed displacements (where the forces are obtained as reactions to those displacements)

The parametric study comprises a base case 1, which contains a circular footing with diameter B=6m and thickness 0.2m, clay layer thickness H_c=0.5B. Sand layer thickness is always H_s=2B which totals to 15m for the default case of B=6m. The computational domain is 100m in diameter (Fig. 7(a)) in order to avoid boundary effects and the element size within 2B from the centre of the footing has been refined to 0.03B, similar to the value of 0.025B used by Wang [9]. In order to adequately capture the VHM mechanisms, the element thickness in the clay layer is 0.2m. A load reference point (RP) is used to set the datum for all loads, moments, displacements and rotations which corresponds to the bottom central point of the footing to avoid adding any pivot arm.

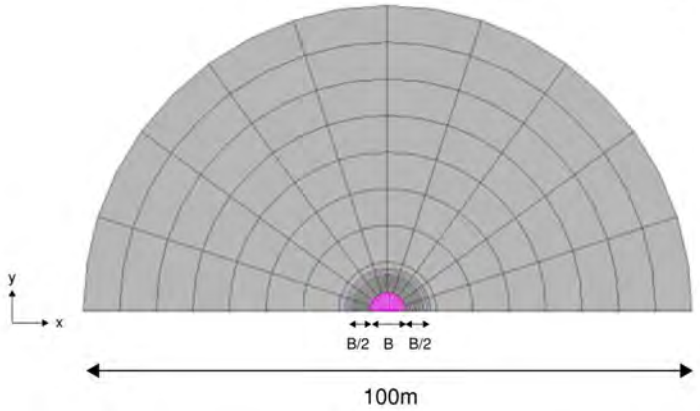

Fig. 7(a) Top view of template mesh

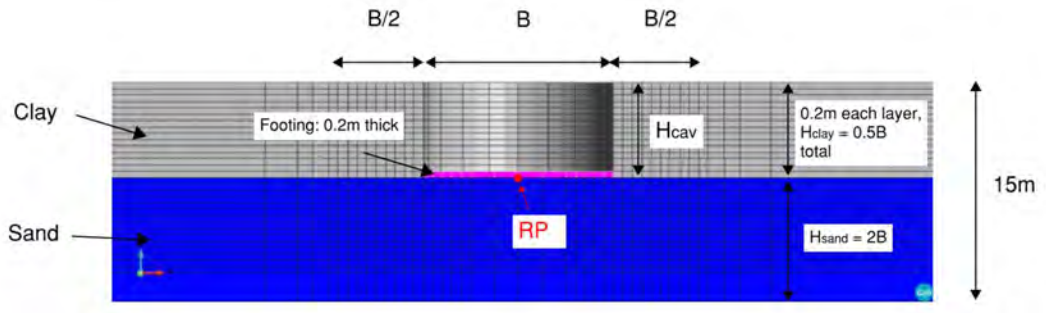

Fig. 7(b) Vertical cross-section through the footing

Material Parameters and Constitutive Models

The top clay layer is modelled with a Tresca constitutive model, while the sand layer underneath is simulated with a Mohr-Coulomb constitutive model. Both of these models are isotropic, linear-elastic perfectly-plastic and when probing the VM envelope, a tension capacity of p' = 5kPa, (p': mean effective stress) was set in order to capture the moment mechanism more accurately and prevent unrealistic tensile stresses mobilising under the footing. The clay layer was modelled as undrained, with a Poisson's ratio of 0.499, while the sand layer was modelled as drained (i.e. the analyses were not hydro-mechanically coupled). To achieve realistic behaviour of spudcan-soil separation, a limiting tensile stresses of p'=5kPa was incorporated into the sand and clay constitutive models. Material properties in the base case are as follows, where only the s_u in the clay and ϕ' in the sand vary in the parametric study:

Clay: $s_u = 30kPa, \gamma' = 8kN/m^3, \nu = 0.499$ (undrained), $E_u = 100{,}000kPa$.
Sand: $c' = 0kPa, \phi' = 25°, \gamma' = 9kN/m^3, \nu = 0.2, E' = 100{,}000kPa$.
Spudcan Footing: $\gamma = 24kN/m^3$, $\nu = 0.2, E = 40 \times 10^6 kPa$. It is noted that the density of the footing is somewhat arbitrary as it has no effect on the results obtained.
K_0 is set to 1 for an isotropic stress field and no dilation angle was modelled in the sand.

Applied displacements

The applied loads and displacements follow the convention sketched in Fig. 8. Vertical and horizontal loading are applied by displacing the entire footing to achieve footing rigidity. Moment loading is performed by holding the vertical displacement of the footing centre constant and the left and right corners of footing are displaced vertically downwards and upwards respectively, resulting in an anticlockwise rotation of the footing.

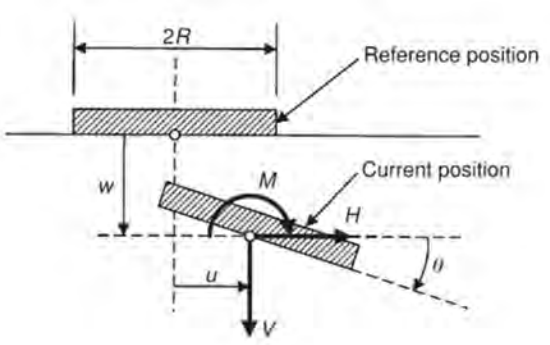

Fig. 8 Schematic of loads and displacements applied to jack-up rig foundation [1]

Parametric study

As currently the combined VH and VM envelopes in the literature for sand are based on surface footings, this parametric study aims to investigate the expected changes in VH and VM bearing capacity envelope size and shape for sand if overlain by clay for a flat circular footing. Investigation of the HM envelope is not within the scope of the current investigation and is conservatively represented by an elliptical shape in ISO 19905-1 [4]. Variables studied under this parametric study are:

1) Case 1-3: Footing diameter, B = 6,12,18m
2) Case 1,4-6: Thickness of clay, H_{clay} = 0.5, 1.0,1.5, 2.0 times the footing diameter, B
3) Case 1,7-8: Undrained shear strength profile of the overlying clay, s_u = 30kPa (homogenous), a normally consolidated profile varying from 2kPa at the seabed surface and increasing at a slope ρ =1.44kPa/m throughout the thickness of the clay layer and $(s_u/\sigma_v')_{nc} = 0.18$, 90kPa (homogenous)
4) Case 1,9-10: Friction angle for the underlying sand, ϕ'- 25,30 and 35 degrees.

The depth of the cavity modelled above the spudcan, H_{cav}, are defined based on the soil strength profile using Formula A.9.3-3 in ISO 19905-1 [4]. If $H_{cav} > H_{clay}$, the cavity is set to be equal to H_{clay}.

RESULTS

Postulated VHM envelope framework for multi-layered and embedded footings

Based on observed VHM envelope shapes in the literature and the analyses performed in this study, it is postulated that the envelope shapes can be classified into three types: parabolic, half parabolic and skewed parabolic, shown in red, blue and green respectively in Fig. 9.

The ISO 19905-1 VHM envelopes will be used as a starting point, as it is founded on top of silica sand and there is no overburden above the foundation. V_0 can be verified by the well-established general bearing capacity equations from Terzaghi (1943) [12] and fitted to field data. The ISO 19905-1 formulation (equation 1) for pure sands gives a symmetrical parabola about $0.5V_0$ and intersects the origin of the VH and VM load space as the vertical tensile capacity is zero as there is no cohesion in the sand.

When the clay-over-sand stratigraphy is introduced, the normalised h_0 and m_0 increases and the envelopes resemble a half parabola. The shape is also slightly right-skewed as the drop off from the peak horizontal or moment load towards the vertical tensile capacity is steeper than the compressive side, agreeing with the envelope shapes as seen in He & Newson (2022) [13], Yun & Bransby (2007) [14] and Wang (2021a) [9], owing to stronger compressive strength of sands. H_0 and M_0 also increase to expand the parabola.

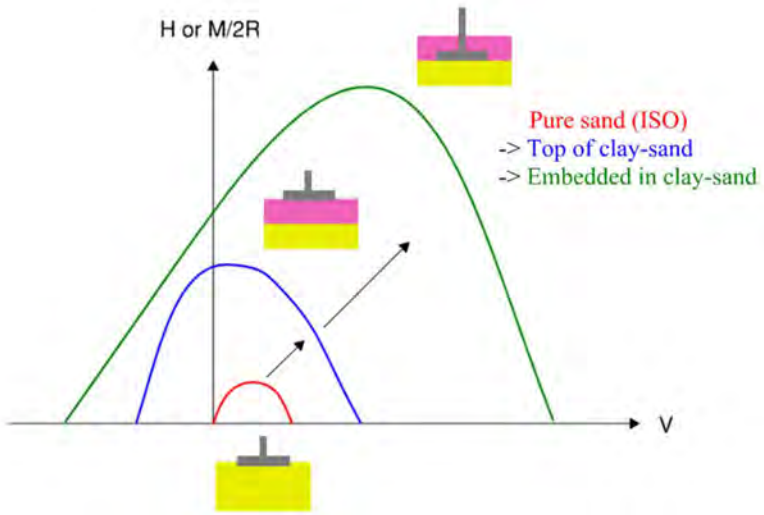

Fig. 9 Explanation of VH and VM envelope shapes in different stratigraphies

VHM mechanisms in clay-over-sand with cavity

VHM mechanisms in the default case (case 1) are shown in Fig. 10(a)-(c), for purely vertical, horizontal and moment mechanisms. These resemble results from Wang (2021a) [9] but the squeezing is not present in clay as the footing is founded directly on sand.

With the cavity removing some or all clay above the footing, depending on the cavity depth calculated, the mechanism is altered from the ones seen in Wang (2021a) [9] (Fig. 6). In the case where there is an open cavity above the footing, the mechanism primarily involves the sand layer. For vertical capacity, this means that clay is only dragged from the cavity wall, and although overbearing in the surrounding clay still exists, direct overburden on the footing is reduced. For horizontal capacity, the smaller vertical loading leads to smaller horizontal frictional resistance from the sand. For moment capacity, the circular scoop failure mechanism is less developed in the clay, mainly appearing in the sand which also leads to a reduction in M_0.

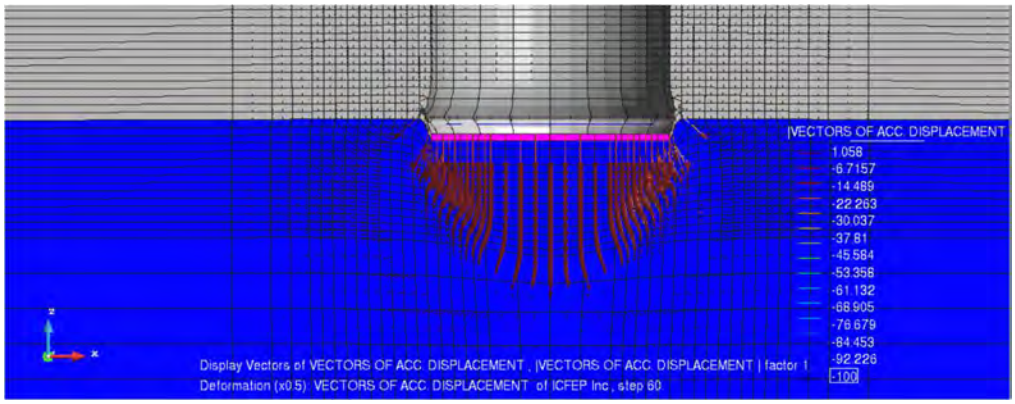

Fig. 10(a) Vertical Mechanism (Case 1), 10x magnification

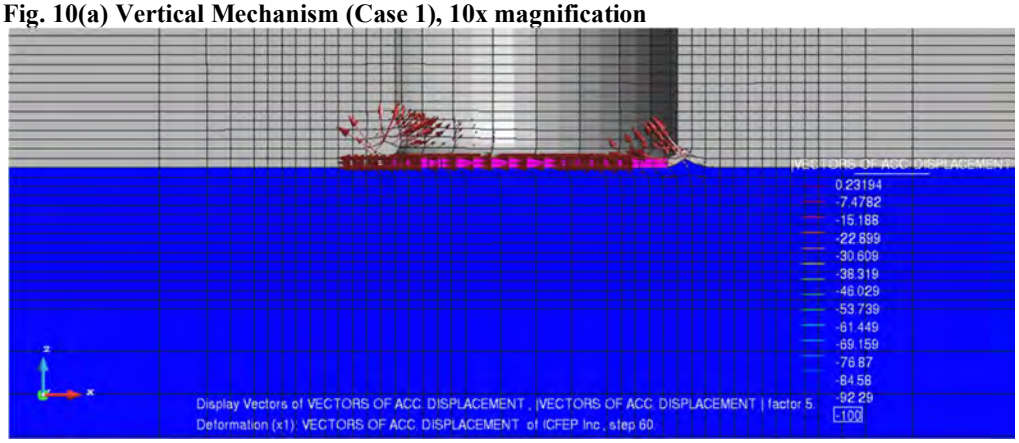

Fig. 10(b) Horizontal Mechanism (Case 1), 1x magnification

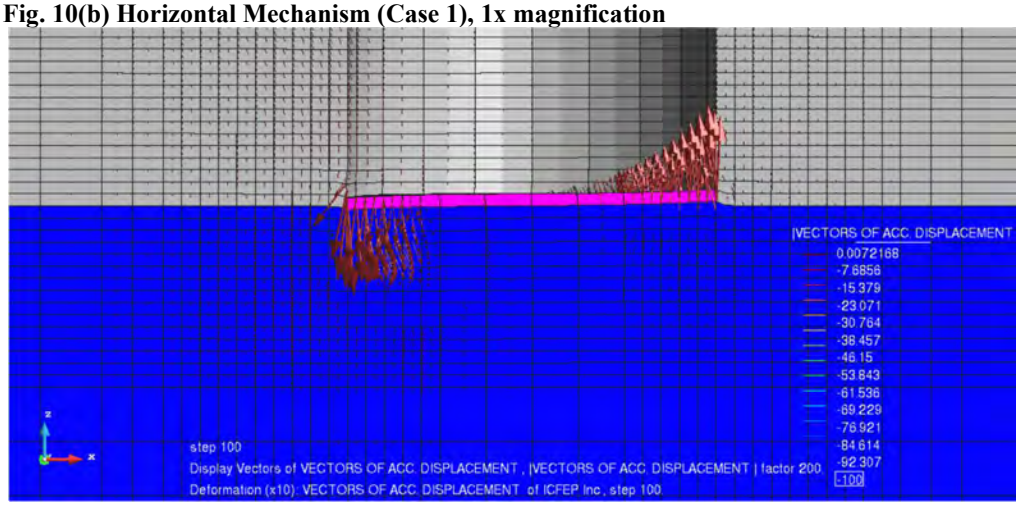

Fig. 10(c) Rotational Mechanism (Case 1), 0.5x magnification

Parametric study results

For comparison between variables, normalised VH and VM envelopes are presented (values in Table 1 and plots in Table 2).The normalised parameters are defined as $v = V/V_0$, $m = M/(2RV_0)$, $h = H/V_0$. In line with ISO 19905-1 [4], normalised factors C_h and C_m are also defined by equations 2a to 2c.

$$Q_{V,net} = Q_V - 0.25\pi B^2 \sigma_v' \quad (2a)$$

$$C_h = H_0/Q_{V,net} \quad (2b)$$

$$C_m = M_0/BQ_{V,net} \quad (2c)$$

where σ_v' is the effective vertical stress.

Case	Parameter Varied	Value	Unit	Q_V (kN)	Q_{Vnet} (kN)	H_o (kN)	$M_o/2R$ (kN)	C_h	C_m
1	B	6	m	32200	31521	4824	4092	0.15	0.13
2	B	12	m	238600	233171	28000	24853	0.12	0.11
3	B	18	m	735000	716678	92198	73572	0.13	0.10
1	H_{clay}	0.5B	-	32200	31521	4824	4092	0.15	0.13
4	H_{clay}	1.0B	-	61800	60443	10565	5130	0.17	0.08
5	H_{clay}	1.5B	-	85800	83764	13308	8744	0.16	0.10
6	H_{clay}	2.0B	-	102000	99286	17461	10217	0.18	0.10
1	s_u	30	kPa	32200	31521	4824	4092	0.15	0.13
7	s_u	2kPa at soil surface, ρ=1.44kPa/m)	kPa	23300	22621	2649	2727	0.12	0.12
8	s_u	90	kPa	36000	35321	7131	4628	0.20	0.13
1	ϕ'	25	deg	32200	31521	4824	4092	0.15	0.13
9	ϕ'	30	deg	59000	58321	7175	7187	0.12	0.12
10	ϕ'	35	deg	102000	101321	10920	12401	0.11	0.12
ISO 19905-1 [4] Values of flat, circular footing on top of sand								*0.12*	*0.075*

Table 1 Summary of the parametric study with comparison to the values provided in ISO 19905-1 [4]

Tests 1-3 vary the footing diameter (B) from 6 to 18m and the clay thickness (H_{clay}) also varies accordingly by 0.5B. The VHM envelope enlarges in size as the contact area is larger, but the normalised envelope (Table 2) shrinks. This is because the gains in vertical component of capacity are larger than the increases in the horizontal and moment capacities as the diameter is increased B.

Tests 1,4-6 vary the clay thickness, H_{clay}, from 0.5B to 2B, in the vertical mechanism this corresponds to a longer shear path and higher overburden, as the cavity depth remains constant at 3.7m, but the clay thickness is increasing (Fig.11).

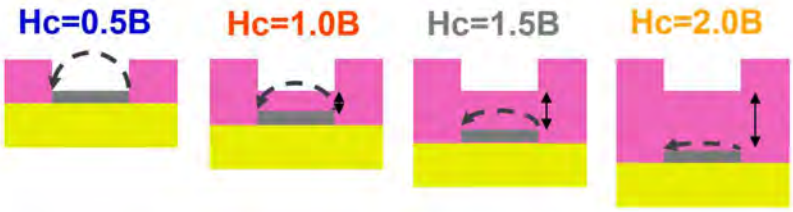

Fig. 11 Increasing clay thickness above footing due to cavity depth and embedment depth in cases 1,4-6

The VHM envelopes increase in size, but the normalised envelopes show different trends in *h*-*v* and *m*-*v* space. For horizontal loading, *h* increases from 0.15 to 0.17, then remains relatively constant. Since the friction mechanism depends on the vertical loading, there is a competing effect of increasing vertical stresses with depth and the effect of the clay cavity depth, which led to a stable value. The normalised moment, however, decreased from 0.13 to 0.08, then increases back to 0.1 when reaching $H_{clay} = 2B$. Since moments mainly depend on the clay parameters above the footing, when $H_{clay} = B$ the cavity is relatively deep compared to cases 5 and 6. The scoop mechanism is relatively unhindered by the thin layer of clay above, which reduces the magnitude of *m*. As the clay layer becomes thicker, the value of *m* increases and stays at 0.1 since the localised scoop mechanism is less sensitive to further increases in the clay thickness above the footing.

Tests 1,7,8 consider a homogenous clay profile of 30kPa, a normally consolidated profile starting at 2kPa with a slope of 1.44kPa/m and a homogenous 90kPa undrained shear strength profile respectively. In the normalised VH envelope a clear trend of increasing from case 7 to 1 to 8 is seen, since the magnitude of the

undrained shear strength in the normally consolidated profile is much smaller than the other two cases, the beneficial effects from the inhomogeneous normally consolidated profile, which gives an additional scoop mechanism near the centre of the footing [2], is outweighed by the lower s_u values. The normalised VM envelopes have less of a clearer trend, as the normally consolidated case (case 7) is still smaller in terms of m than the homogenous cases, the 30 and 90kPa cases have similar peaks. This is due to the cavity in the clay being the same depth for the homogenous cases, which removes the added direct overburden on top of the footing. The scoop mechanism is practically determined by sand properties if the cavity goes through the entire clay layer (i.e. an open void above the footing) as the plastic strains do not extend into the clay layer except for some localised zones near the footing's circumference. The contribution from the clay undrained shear strength is therefore minimal. The cavity depth in the normally consolidated case, on the other hand, is shallower due to the slope of the s_u profile. The added shearing through the clay above the footing is shown to only decrease the normalised m to only 7% smaller than the homogenous cases, despite the much smaller magnitude of s_u in the clay above.

Tests 1, 9, 10 vary the angle of shearing resistance in the sand from 25° in Test 1 to 30° and 35° respectively. As expected, the VHM envelope expands due to the additional sand bearing capacity. The horizontal capacity is also affected by the increase in friction angle owing to the mechanism being frictional in nature. The normalised h decreases sharply from 0.15 to 0.11. The normalised m is again less sensitive to this change, only decreasing from 0.13 to a value of 0.12 for both ϕ'=30° and 35°. Although the scoop mechanism cuts through the sand, the mechanism is in principle a shearing one and similar in nature to that of the vertical loading. The increase of V_0 and M_0 is much more proportional and hence gave rise to minimal changes when ϕ' is varied.

Shapes of the normalised VH and VM envelopes are shown in Table 2, which agree with the proposed framework and other literature previously mentioned.

DISCUSSION

With the results of the parametric study, the framework established in the previous section can now be used to relate the individual deformation mechanisms in the clay-sand setting to the combined VHM envelope. This can replace full 3D numerical simulations with a simpler model that can be implemented into pushover structural analyses of the jack-up rig. The shape of the VHM envelopes are shown in Fig. 9, which changes from parabolic and intersecting the origin (pure sand), half parabolic and gains tensile capacity (surface on clay-over-sand), skewed parabolas (embedded clay-over-sand).

This implies that the typical parabolic ellipsoid often used as the default normalised yield surface shape in single-layered soils, cannot be simply applied to multi-layered stratigraphies. The apex for minimum vertical loading also does not coincide at the VHM origin, rather, it is shifted towards the negative vertical load axis due to the presence of embedment. In future studies, HM envelopes can be traced to pinpoint the size and eccentricity of the elliptical yield surface at low vertical loading since the VH envelopes clearly indicate a negative vertical intercept, but the moment tests are inconclusive. Intuitively the VH and VM envelopes should meet at the same point on the vertical axis.

Previous literature that have only investigated a footing for an offshore jack-up rig have mainly focused on one type of soil such as clay or sand and are founded on the seabed level. This ignores the added contribution of more complicated failure mechanisms of the clay-sand layers which is often found in-situ and also overlooks the effect of embedment.

The values provided in ISO 19905-1 [4] only estimate the vertical capacity of pure sands or clay, which is rarely the case in the field. By comparing vertical capacity of cases 1-10 in clay over sand to the corresponding Q_V by the guideline formulas with the same footing geometry, differences of 9% in case 10 to 57% in case 8 are observed. This is also seen in the VHM envelopes where the ISO 19905-1 [4] vertical bearing capacities are lower than those found by the finite element analyses. The values of h and m were taken from a selection of datasets within the technical literature and the H_0/V_0 and M_0/BV_0 ratios were likely to be chosen so as to be slightly on the conservative side. Furthermore, they do not attempt to account for the beneficial effects of embedment in layered soil profiles and consequently are observed to underpredict the peak of the VHM envelopes in clay over sand. This extra capacity is significant in the context of offshore design, therefore, this added capacity from stratigraphy alone should be incorporated into site assessments as a combination of sand and clay strata can be beneficial. This is because the mechanisms, especially for vertical and moment can be disrupted by altering the load path due to soil inhomogeneity.

Case	VH	VM
1-3 (B)	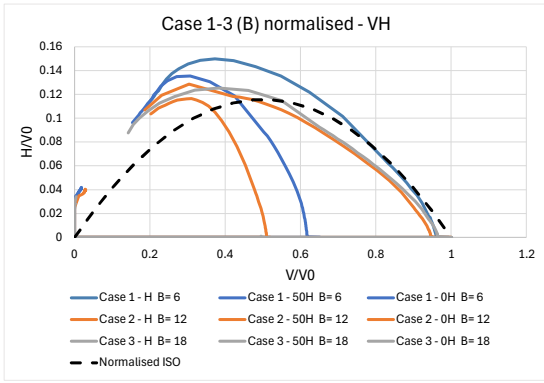	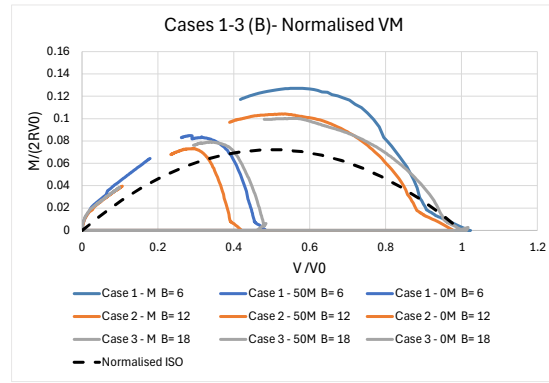
1, 4-6 (Hc)	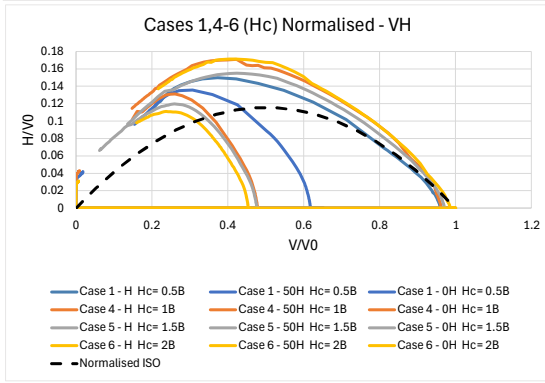	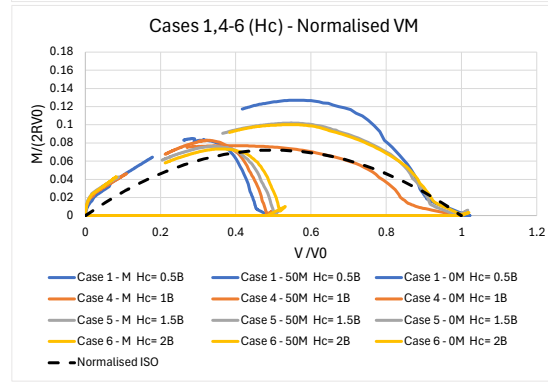
1, 7-8 (su)	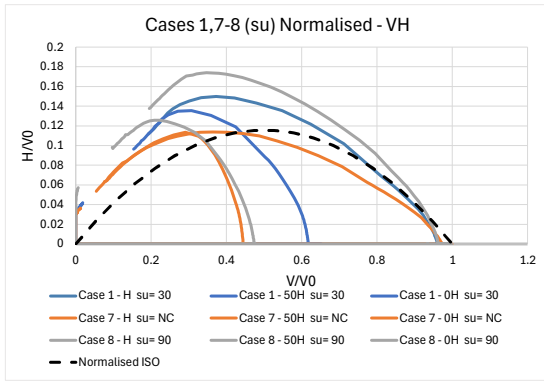	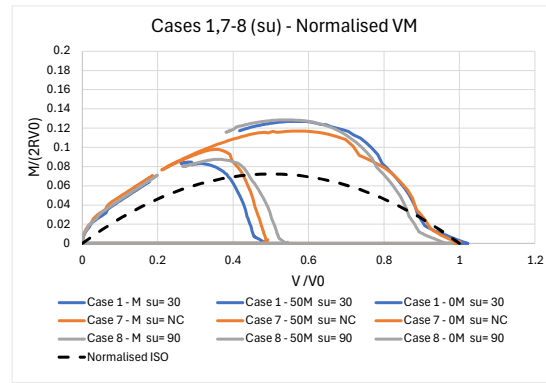
1, 9-10 (ϕ')	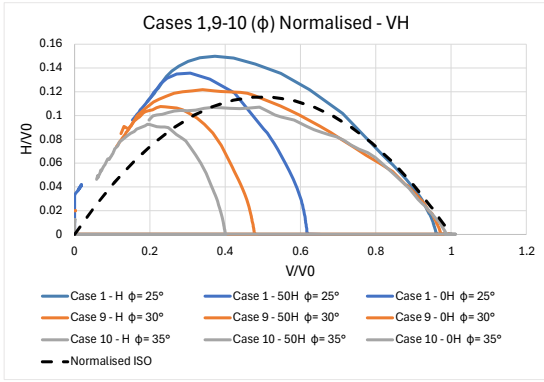	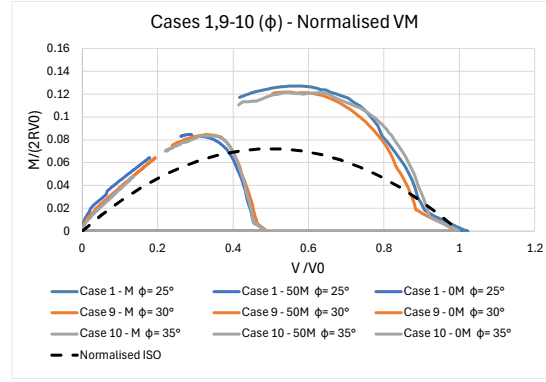

Table 2 Normalised VHM envelopes of the parametric study

Another observation from the VHM envelopes is that parameters that increase the VHM capacities do not continue their trends indefinitely and are attributed to the parameter's respective role in the mechanisms. This can be observed from the normalised envelopes (Table 2). For footing diameter, increasing B from 6 to 18m gave smaller yield surface sizes. This is because the individual V, H and M components of capacity increase at different rates with respect to increases in the footing diameter with the horizontal and moment capacities increasing by a smaller amount compared to the vertical capacity. This then causes the normalised envelope to shrink. With respect to the thickness of clay, as the footing is embedded in deeper clay layers, the overburden stresses are increasing. The normalised VH envelope expands with thicker clay but the normalised VM envelope shrinks. For horizontal capacity, the movement induces shearing within the overlying clay, which increases with a greater thickness of clay above the foundation. The normalised moment capacity however decreases because the maximum tensile soil stresses under the footing is capped at 5kPa for both clay and sand for all clay thicknesses, which limits the available moment resistance to footing rotation. Overburden mainly increases the compressive strength of the sand, but not so much the tensile strength, so when calculating the moment values the tensile contribution to moment capacity will not increase as much as vertical capacity, leading to a smaller normalised VM yield surface.

Overall the normalised moment capacity is seen to be less sensitive to the parameters varied in this study than the normalised horizontal capacity. This is commonly seen in other studies.

Limitations of this study include a lack of information for the HM envelope, to define the elliptical shape and eccentricity to fully complete the three-dimensional VHM envelope. Flow rule and hardening laws have not been derived in this study. The present analyses have not attempted to capture detailed soil backflow and cavity collapse mechanisms as the spudcan penetrates, which could provide a more accurate picture of the soil-structure interaction.

A future direction of this research could be to expand to sand-over-clay or three-layer stratigraphies, which consider sand plug mechanisms that also contribute to the VHM capacity. Curve-fitting can also be performed on this parametric study if a wider range and types of parameters are included such that quantitative plasticity-based frameworks can be established for future offshore jack-up rig assessments.

CONCLUSIONS

In this paper, vertical-horizontal (VH) and vertical-moment (VM) bearing capacity envelopes for a circular footing used in offshore jack-up rigs are investigated using 3D numerical modelling. The foundations are embedded at the interface between a sand layer overlain by clay, which is often encountered in practice. Various factors such as footing size, clay thickness, clay and sand strength parameters have been investigated by a parametric study.

Results indicate that the multi-layered setting and embedment provides additional foundation capacity as compared to a fully clay or sand scenario as the change in soil strengths at the interface gives altered loading paths and expands the yield envelopes. Moreover, these beneficial effects have been summarised as a postulated framework for the yield surface shape when changing the soil layers from pure sand, surface clay-sand and embedded clay-sand and relates the individual mechanisms in vertical, horizontal and moment loading to the ultimate bearing capacity. By accounting for the findings from this study, more accurate predictions of foundation bearing capacity in offshore construction can be achieved for more optimised site assessments in the future.

REFERENCES

[1] Gottardi, G., Houlsby, G.T. and Butterfield, R., (1999). Plastic response of circular footings on sand under general planar loading. *Geotechnique*, 49(4), pp.453-469.

[2] Martin, C.M. and Houlsby, G.T., (2000). Combined loading of spudcan foundations on clay: Laboratory tests. *Geotechnique*, 50(4), pp.325-338.

[3] Wang, Y., Cassidy, M.J. and Bienen, B., (2020). Numerical investigation of bearing capacity of spudcan foundations in clay overlying sand under combined loading. *Journal of Geotechnical and Geoenvironmental Engineering*, 146(11), p.04020117.

[4] ISO (2023). *ISO 19905-1: Oil and gas industries including lower carbon energy - Site-specific assessment of mobile offshore units - Part 1: Jack-ups: elevated at a site*. Third edition. International Organization for Standardization, Geneva, Switzerland.

[6] Tan, F. (1990). *Centrifuge and theoretical modelling of conical footings on sand*. PhD Thesis, University of Cambridge.

[7] Gottardi, G., Houlsby, G.T., & Butterfield, R. (1995). *Yield loci for shallow foundations by swipe testing*. *Geotechnique*, 45(4), pp. 749–753. Thomas Telford Publishing, London, UK.

[8] Gottardi, G., Houlsby, G.T., & Butterfield, R. (1999). *The behaviour of circular footings on sand under general planar loading*. *Geotechnique*, 49(4), pp. 453–469. Thomas Telford Publishing, London, UK.

[9] Wang, Y., (2021a). Evaluating spudcan VHM behavior in clay over sand. PhD thesis, University of Western Australia, Perth, Australia.

[10] Potts, D.M. and Zdravkovic, L., (1999). Finite element analysis in geotechnical engineering: Theory. Thomas Telford Publishing, London, UK.

[11] Potts, D.M. and Zdravkovic, L., (2001). Finite element analysis in geotechnical engineering: Application. Thomas Telford Publishing, London, UK.

[12] Terzaghi, K., (1943). *Theoretical Soil Mechanics*. John Wiley & Sons, New York.

[13] He, X. and Newson, T., (2022). Undrained capacity of circular shallow foundations under combined VHMT loading. *Géotechnique Letters*, 12(2), pp.1-15.

[14] Yun, G. and Bransby, M.F., (2007). The horizontal–moment capacity of embedded foundations. *Geotechnique*, 57(8), pp.713-722.